

On the inverse identification of sheet metal mechanical behaviour using a heterogeneous Arcan virtual experiment

HENRIQUES Joao^{1,2,a*}, ANDRADE-CAMPOS António^{1,2,b} and XAVIER José^{2,3,c}

¹Centre for Mechanical Technology and Automation (TEMA), Department of Mechanical Engineering, University of Aveiro, Campus Universitário de Santiago, 3810-193 Aveiro, Portugal

²Intelligent Systems Associate Laboratory (LASI), 4800-058 Guimarães, Portugal

³Research and Development Unit for Mechanical and Industrial Engineering (UNIDEMI), Department of Mechanical and Industrial Engineering, NOVA School of Science and Technology, NOVA University Lisbon, 2825-149 Lisbon, Portugal

^ajoaodiogofh@ua.pt, ^bgilac@ua.pt, ^cjmc.xavier@fct.unl.pt

Keywords: Sheet Metal Forming, Anisotropic Plasticity, Arcan Test, Heterogeneous Test Evaluation, Inverse Identification, Digital Image Correlation, Synthetic Images

Abstract. Modelling and simulation are critical stages of product development in modern industry. Simulation tools in solid mechanics use constitutive models and their parameters to describe the behaviour of materials. Nowadays, with the use of heterogeneous test configurations and full-field measurements, it is possible to measure a combination of multiple strain states, allowing for the identification of multiple parameters from a single test with reduced cost and time. This work aims to investigate the potential for obtaining heterogeneous states of strain/stress with the Arcan test configuration. A finite element model was developed using a specimen with a smooth arc section in which the loading and material directions varied, producing tensile, shear, or mixed mode responses. The most heterogeneous test configuration was selected using a heterogeneous criterion and the numerical results were used to generate synthetic speckle pattern images and further processed by digital image correlation (DIC). The DIC results were used as input for the identification procedure through the virtual fields method (VFM) for the simultaneous calibration of the Swift hardening law and the Hill'48 anisotropic yield criterion. The identified solution was compared with the ground truth material parameters. The results show the potential of combining the Arcan test with the VFM to simultaneously identify material parameters for anisotropic plasticity models of sheet metals.

Introduction

Computer-aided engineering systems are a powerful tool used in modern industry to optimise costs and time consumption in the design of new products. Nowadays, in metal forming technology, the development of sheet metal parts tends to be more virtual through the use of numerical simulation. Sheet metal anisotropy is a critical property that greatly influences the accuracy of the numerical results [1]. This anisotropy is a result of the rolling process that produces preferential orientations in the material texture [2], which induces differences in the yield stress along different orientation angles from the rolling direction (RD). Therefore, the accuracy of the simulation is heavily reliant on the calibration of the model that describes the behaviour of the materials during the forming process including the anisotropy. The improved accuracy of complex constitutive models is related to increased flexibility in the mathematical formulation, which translates to a greater number of constitutive parameters to calibrate, resulting in increased calibration complexity [3]. Classically, the calibration procedure was done using standard homogeneous tests [4]. However, as models become more accurate and complex, their calibration has become a difficult task, increasing the number of experimental tests required to accurately calibrate such models.



Recent developments in optical full-field measurement techniques, such as digital image correlation (DIC) [5], have been changing the approach to the calibration procedure of material constitutive models. The increased amount of measurable kinematic data has enabled the transition from simple statically determinate tests to innovative tests with complex geometries that produce heterogeneous states of stress and strain, allowing for the collection of more data and thus reducing the experimental effort [6]. However, there is no closed-form formulation relating local kinematic data to constitutive parameters. As a result, in recent years, there has been an increased interest in the development of robust inverse identification techniques, most notably the virtual fields method (VFM) [7] and the finite element model updating (FEMU) method [8]. These approaches have altered the way mechanical tests are conducted, eventually leading to the development of new standards as cameras gradually replace strain gauges and extensometers in both academia and industry. Nonetheless, the ability to reduce the number of experimental tests required to simultaneously identify material parameters is highly dependent on the test configuration used, which implies that optimised test configurations are required to fully benefit from this new paradigm [6,9].

The mechanical testing scientific community has made significant efforts in recent years to find methodologies for developing optimised specimens [6]. There has been an increase in the development of heterogeneous tests through different methodologies, for instance, using empirical knowledge [10,11] or numerical optimisation procedures [9,12,13]. The specimen design by empirical knowledge is tied to the author's previous experience. However, this approach frequently results in unoptimised specimen shapes, especially when using complex constitutive models, since the relationship between the constitutive parameters and strain measurements can be quite complex [6]. A more logical approach that permits the use of various design variables is the use of numerical optimisation procedures. The design variables can range from the strain states [4,9], identification quality [14] or full-identification chain quality [15,16]. For a more comprehensive review of the state-of-the-art of heterogeneous specimen design, the reader is referred to the work of Pierron and Grédiac [6].

The Arcan test is an interesting test configuration since it allows varying the loading direction in a standard uniaxial tensile testing machine. In the framework of sheet metal plasticity, the majority of the previously mentioned authors focused on optimising the shape of the specimen or using geometries with holes or notches. However, changing the loading direction can also be used to increase strain heterogeneity, which in the case of the Arcan test can result in tension, shear or mixed mode responses. Wang *et al.* [15,16] designed orthotropic foam tests using the Arcan fixture by varying the loading direction and the material orientation. The authors were able to successfully calibrate the orthotropic linear elastic constitutive model with a single test when using the optimised design parameters. Although some authors used the Arcan test in sheet metal plasticity [17,18], it is seldom used in heterogeneous test design for the calibration of plastic constitutive models. Nonetheless, the Arcan test has the potential to provide interesting heterogeneous test configurations when used for test design in sheet metal plasticity.

The goal of this work is to evaluate the heterogeneity of stress/strain states for different Arcan test configurations using a specimen with a smooth arc section [18]. A finite element model was developed in which the loading and material directions varied, producing tensile, shear, or mixed mode responses. The reference constitutive parameters for the DP600 steel were used [19] to select the most promising test configuration using a heterogeneous criterion [4,12]. To get closer to real experimental data, the FEA results for the most heterogeneous test configuration were used to generate synthetic speckle pattern images, which were further processed by DIC. The parameters for the Hill'48 yield criteria and the Swift hardening law were simultaneously identified using the VFM and compared to the ground truth parameters.

Methodology

Numerical model.

In this work, a finite element model of the Arcan test was developed using a specimen with a smooth arc section [18] under quasi-static loading conditions. The load direction angle (α) and the RD angle (θ) with the x -axis were varied, producing tensile, shear, or mixed mode responses. The angles θ and α assumed the values of 0° , 45° or 90° , totalling nine possible test configuration combinations. The finite element model was implemented in ABAQUS/Standard software [20] assuming plane stress conditions and a thickness of 0.8 mm for the specimen. A mesh convergence study was performed and a total of 2596 four-node plane stress elements (CPS4R) were used with displacement-driven loading conditions. The forming limit curve (FLC) is used as the rupture criteria and the test was conducted until the failure of the specimen with a total of 40 load steps. Fig. 1a depicts the specimen geometry and dimensions (in mm) and Fig. 1b shows the FEA mesh and boundary conditions, including the variation of the material and load direction angles.

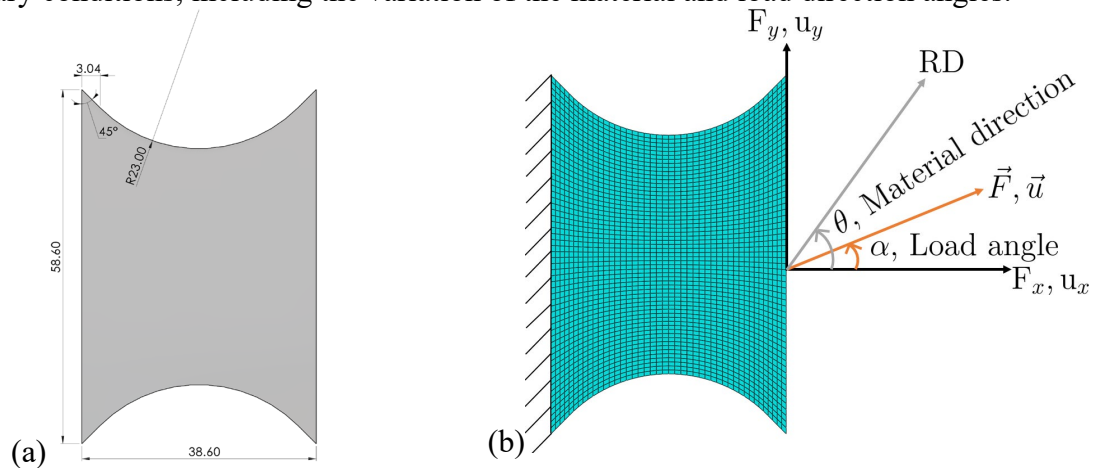


Fig. 1. (a) Geometry and dimensions [mm] of the specimen with smooth arc section [18], (b) Finite element mesh and boundary conditions, showing the variation of the material and load direction angles.

Material and constitutive model.

A sheet metal of DP600 dual-phase steel with 0.8 mm thickness was considered in this work. The elastoplastic behaviour of the material was modelled using phenomenological models, namely isotropic elasticity described by Hooke's law ($E = 210$ GPa and $\nu = 0.3$) and anisotropic plastic behaviour described by the Hill'48 yield criteria [21] and Swift hardening law. The reference parameters of the DP600 steel [19] are presented in Table 2. In this work, the commonly used condition $G+H=1$ is assumed [3], which deduces that the yield stress in the rolling direction corresponds to the yield stress (σ_y). A user-defined material subroutine, Unified Material Model Driver for Plasticity (UMMDp) [22], was used to model the material behaviour.

Test evaluation.

The selection of the most heterogeneous test configuration is not an obvious task. Therefore, two heterogeneity indicators were used to evaluate the richness of strain/stress in each of the test configurations used. The first indicator was initially proposed by Souto *et al.* [4], and is based on the maximization of five quantities that the ideal test should exhibit and can be written as:

$$IT_1 = w_{r1} \frac{\text{Std}(\varepsilon_2/\varepsilon_1)}{w_{a1}} + w_{r2} \frac{(\varepsilon_2/\varepsilon_1)_R}{w_{a2}} + w_{r3} \frac{\text{Std}(\bar{\varepsilon}^P)}{w_{a3}} + w_{r4} \frac{\bar{\varepsilon}_{\max}^P}{w_{a4}} + w_{r5} \frac{\text{Av}(\bar{\varepsilon}^P)}{w_{a5}}, \quad (1)$$

where ε_1 and ε_2 are the major and minor principal strains, respectively, $\bar{\varepsilon}^P$ is the equivalent plastic strain, $\bar{\varepsilon}_{\max}^P$ is the averaged maximum value of the equivalent plastic strain for each stress/strain state and w_r , w_a are relative and absolute weighting factors, respectively. Since the ratio between

the minor and major principal strains represents various strain states, the first two quantities presume that its distribution should be as wide as possible. The final three quantities are related to the equivalent plastic strain, which should be as heterogeneous and widely distributed as possible, as well as have a high global plastic strain level. The quantities are further normalised and adjusted in terms of importance according to the different weights. The weights used in this work were the recommended from the original work by Souto *et al.* [4] and are presented in Table 1.

Table 1. Absolute and relative weighting factors used for the definition of IT_1 [4].

w_{a1}	w_{a2}	w_{a3}	w_{a4}	w_{a5}	w_{r1}	w_{r2}	w_{r3}	w_{r4}	w_{r5}
1	4	0.25	1	1	0.3	0.03	0.17	0.4	0.1

The second heterogeneity indicator is the rotation angle (γ) which evaluates the sensitivity of the specimen to anisotropy and is based on the principal angle formulation [23]. This indicator varies between 0° and 90° and represents the principal direction for the maximum principal stress in absolute value and can be written as:

$$\gamma = \begin{cases} 45 & \text{if } \sigma_{11} = \sigma_{22} \text{ and } \sigma_{12} \neq 0 \\ 45(1 - q) + q|\beta| & \text{otherwise} \end{cases}, \quad (2)$$

where σ_{11} , σ_{22} , σ_{12} are the components of the Cauchy stress tensor in the material coordinate system and β is the principal angle in degrees and q is an integer that assumes the value of 1 or -1 that can be calculated from:

$$q = \frac{\sigma_{11} - \sigma_{22}}{|\sigma_{11} - \sigma_{22}|} \frac{|\sigma_1| - |\sigma_2|}{||\sigma_1| - |\sigma_2||}, \quad (3)$$

where σ_1 , σ_2 are the major and minor principal stresses, respectively. The formulation is written in such a way that it can represent most of the conceivable stress/strain states in Mohr's circle [23], except for being undefined in the purely biaxial stress state ($\sigma_{11} = \sigma_{22}$ and $\sigma_{12} = 0$).

Synthetic images and digital image correlation.

The numerical results of the most heterogeneous test configuration were used to synthetically deform a speckle pattern image using the FE Deformation module from the MatchID software [24]. The synthetic speckle pattern images were then further processed with the subset-based 2D-DIC using the MatchID software [24]. The goal of this approach is to simulate a real experiment in which the results are measured by using the DIC filter, where spatial averaging is used to reduce the inherent experimental noise. This approach makes it possible to capture the full uncertainty propagation through the identification chain and leads to more realistic identification results that can also be applied to test design [6].

Furthermore, the choice of DIC settings has a significant impact on measurement accuracy [8]. Therefore, the MatchID Performance Analysis module [24] was used to analyse several combinations of these settings in order to find a good balance between spatial resolution and accuracy. The hardware and DIC settings used here are equal to those used in a previous work (see [25]).

Virtual fields method.

The material constitutive parameters were identified using the VFM, which is based on the principle of virtual work. The objective function for the VFM can be written in static conditions while ignoring body forces as:

$$R = \left(- \int_V \boldsymbol{\sigma}(\boldsymbol{\chi}, \boldsymbol{\varepsilon}) : \text{grad } \mathbf{u}^* dV + \int_{\partial V} \mathbf{T} \cdot \mathbf{u}^* dS \right)^2 \approx 0, \quad (4)$$

where R is the residual, $\boldsymbol{\sigma}$ is the Cauchy stress tensor which is a function of the material parameter set $\boldsymbol{\chi}$ and the strain tensor $\boldsymbol{\varepsilon}$, and \mathbf{u}^* is the virtual displacement vector. The internal virtual work is then calculated for the volume V of the given solid. \mathbf{T} is the traction vector acting on the boundary of the solid and ∂V is the boundary where the loading is applied.

The idea behind the use of VFM for the identification of constitutive parameters is to find the material parameters set that minimises the gap between the internal and external virtual works. Another important aspect of VFM is the selection of appropriate virtual fields \mathbf{u}^* , which can be done either manually or automatically. The manual selection of the virtual fields is done by user experience. These must, however, meet the following requirements: (i) \mathbf{u}^* must be kinematically admissible, (ii) \mathbf{u}^* should be constant at the boundary ∂V , in order to use the global force rather than its distribution, which is unknown in experimental tests and (iii) \mathbf{u}^* must be collinear with \mathbf{T} to eliminate components of the loading forces that are unknown [3]. For more details on automatic strategies for the selection of virtual fields see [26,27].

Results and Discussion

Test evaluation. The IT_1 heterogeneity criterion was calculated using the numerical results of each test configuration. To simplify the evaluation, only the results from the last increment before failure were used, since these are a good indication of the stress and strain states observed in a specimen under monotonic loading [4,23]. Each term of the IT_1 criterion was also evaluated separately to see the relative advantages of each test configuration. Fig. 2 depicts the results computed for the IT_1 criterion as well as each of its terms as a function of the load angle (α) for each RD angle (θ).

The results indicate that the shear test configurations ($\alpha=90^\circ$) are the most heterogeneous, owing to the higher standard deviation of the ratio between the minor and major principal strains, as well as the higher average and maximum value of the equivalent plastic strain. Tensile test configurations ($\alpha=0^\circ$), on the other hand, provide the least amount of information about the mechanical behaviour of the material, which is not surprising given the relatively simple specimen geometry used, which promotes primarily the tensile stress/strain state localised in a narrow area of the specimen. According to the results, the mixed-mode response test configuration ($\alpha=45^\circ$) provides more information about the material's mechanical behaviour than the tensile test configurations, but it is still less heterogeneous than the shear test configurations. Furthermore, it can be seen that the shear test configuration with the 90° RD ($\theta=90^\circ$) gives the most information regarding the mechanical behaviour of the material in accordance with the criteria being used. This is primarily due to the larger equivalent plastic strain, average and standard deviation values.

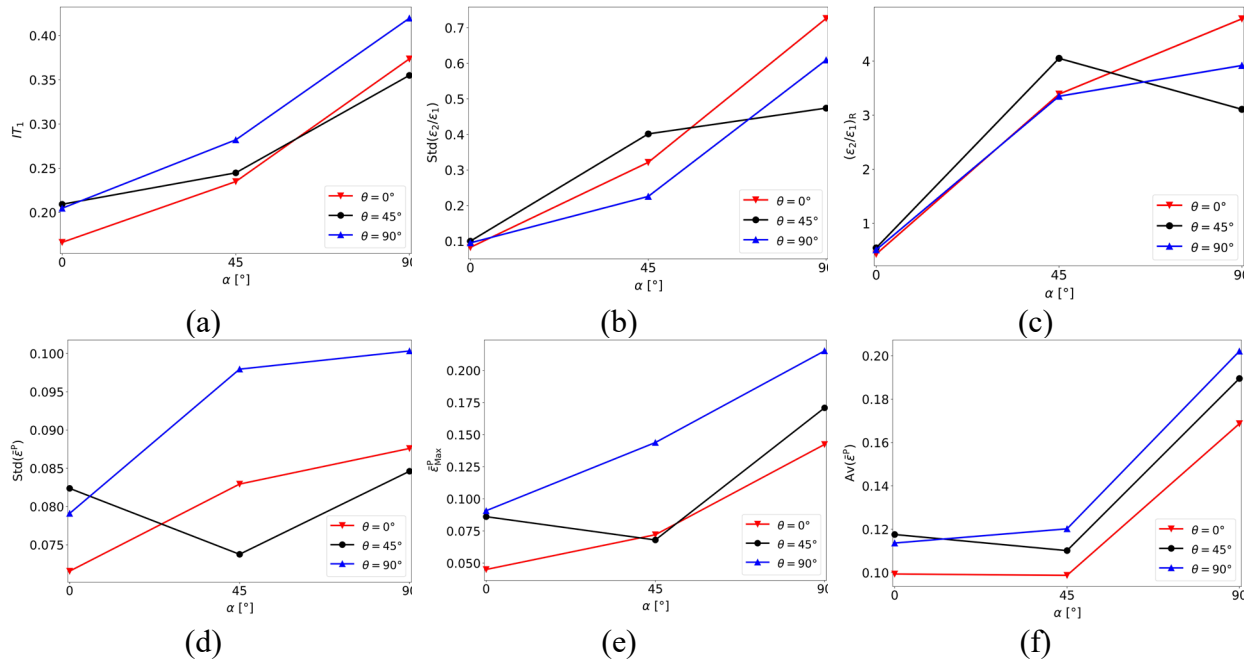


Fig. 2. Mechanical test heterogeneity indicator results for all test configurations: (a) IT_1 , (b) $Std(\epsilon_2/\epsilon_1)$, (c) $(\epsilon_2/\epsilon_1)_R$, (d) $Std(\bar{\epsilon}^P)$, (e) $\bar{\epsilon}_{max}^P$ and (f) $Av(\bar{\epsilon}^P)$.

A qualitative analysis was also carried out by investigating the major and minor principal stresses and strains as well as the rotation angle criterion for the most heterogeneous test configuration of each assessed load angle (see Fig. 3).

According to the principal strains and stresses diagrams, the shear load test with $\theta=90^\circ$ exhibits the greatest variety of stress/strain states, ranging from uniaxial compression to pure shear to uniaxial tension. The other test configurations, on the other hand, mostly provide the uniaxial tension state, with the uniaxial tensile test configuration approaching plane strain tension. These qualitative results support the previous analysis using the IT_1 criterion, which indicates that the shear load test configuration is the most heterogeneous, with a higher standard deviation in the ratio between the principal strains.

It is also interesting to locate the material points of higher equivalent plastic strain in both strain and stress diagrams, the rotation angle histogram and the contour represented in the specimen geometry inside the rotation angle diagram. For instance, in Fig. 3a, the points with the highest equivalent plastic strain are in the specimen's centre and are primarily in the uniaxial tension state, with rotation angles ranging from 30° to 60° . According to the rotation angle histogram results, the material points for the loading angles of 45° and 90° (Figs. 3b and 3c) are primarily on the right side (between 45° and 90°), with some points also on the left side of the histogram, but with low levels of equivalent plastic strain, and in the case of the test with a loading angle of 45° , they still are in the elastic regime. On the other hand, the rotation angle histogram for the tensile load test (Fig. 3a) shows a wide distribution of points, with the highest equivalent plastic strain occurring between 30° and 60° , which indicates that this test may be the most sensitive to anisotropy out of the three tests investigated in this qualitative analysis.

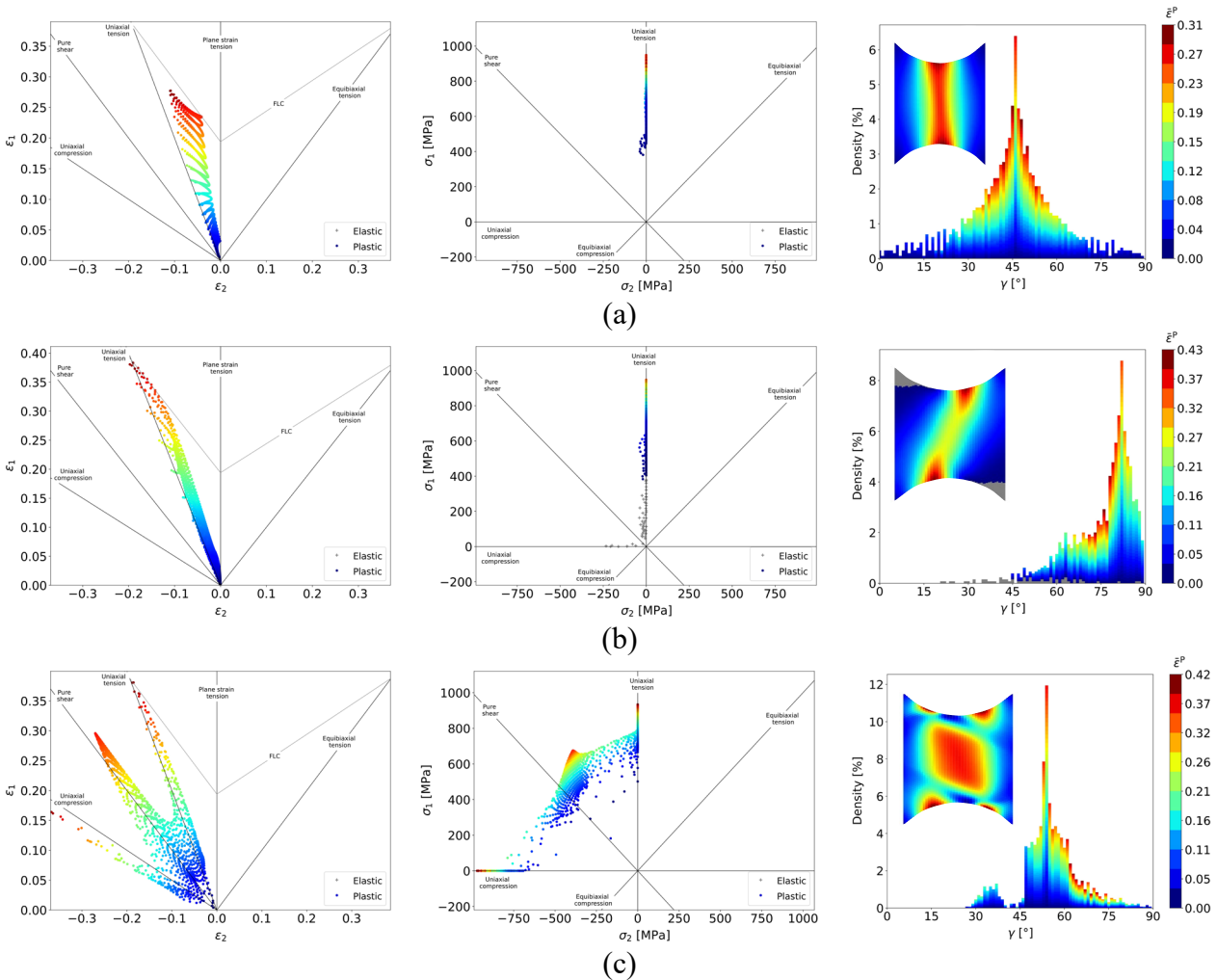


Fig. 3. Numerical results regarding principal strains diagram (left), the principal stresses diagram (center) and rotation angle (right) for the most heterogeneous test configuration of each load angle: (a) $\alpha = 0^\circ$ and $\theta = 45^\circ$, (b) $\alpha = 45^\circ$ and $\theta = 90^\circ$ and (c) $\alpha = 90^\circ$ and $\theta = 90^\circ$.

While it can be difficult to quantitatively rank all the test configurations, the test with a loading angle of 45° can generally be considered to be the least interesting one. The shear load test appears to outperform the tensile load test in the heterogeneity of strain/stress states. However, the opposite can be said about the rotation angle distribution. Nonetheless, the shear load test with the 90° RD was chosen for the identification process due to significantly higher performance in the stress/strain states and IT_1 criterion results, despite having a narrower distribution of the rotation angle.

Inverse identification.

The numerical results of the shear load test with the 90° RD were used to generate synthetic speckle images, which were then processed by DIC. The DIC results were then used for the inverse identification with VFM with one uniform virtual field, using the VFM module from the MatchID software [24]. Four identification runs were carried out, each with a unique initial set of parameters that were generated using the Latin hypercube sampling (LHS) method. Table 2 lists the reference parameters for the DP600 steel [19], the lower and upper bounds for each parameter, the initial set of parameters used for each identification run, the residual value, the identification results and the absolute relative error.

Table 2. Reference [19] and initial set of parameters, lower and upper bounds, identification results, final residual value and absolute relative error of each of the identification runs.

	F	G	H	N	K [MPa]	ϵ_0	n
Ref. parameters	0.3748	0.5291	0.4709	1.1125	979.46	0.00535	0.194
Lower bound	0.2624	-	0.3296	0.7787	685.62	0.00370	0.136
Upper bound	0.4872	-	0.6122	1.4462	1273.30	0.00700	0.252
Run 1 - Final residual = 0.6632							
Initial parameters	0.3467	-	0.4356	1.3628	759.08	0.00580	0.238
Id. parameters	0.4185	0.6697	0.3303	1.2970	1054.00	0.00534	0.199
Relative error [%]	11.66	26.57	29.86	16.58	7.61	0.19	2.58
Run 2 - Final residual = 0.7142							
Initial parameters	0.4591	-	0.5769	1.0290	1052.92	0.00490	0.179
Id. parameters	0.3925	0.6699	0.3301	1.25	1036	0.00559	0.201
Relative error [%]	4.72	26.61	29.90	12.36	5.77	4.49	3.61
Run 3 - Final residual = 0.4432							
Initial parameters	0.2905	-	0.5062	0.8621	906.00	0.00410	0.209
Id. parameters	0.4872	0.6704	0.3296	1.4280	1086.00	0.00371	0.1875
Relative error [%]	29.99	26.71	30.01	28.36	10.88	30.65	3.35
Run 4 - Final residual = 0.8209							
Initial parameters	0.4029	-	0.3649	1.1959	1199.84	0.00660	0.150
Id. parameters	0.4872	0.6704	0.3296	1.2430	1043.00	0.00700	0.209
Relative error [%]	29.99	26.71	30.01	11.73	6.49	30.84	7.73

The results show that the identified constitutive parameters related to the swift hardening law have a lower absolute relative error than the results for the Hill'48 anisotropy yield criterion. This was expected, given that the qualitative analysis conducted previously indicated that this test configuration contained richer information regarding the stress/strain states than the material anisotropy. Though the difference in residual between all the identification runs was relatively low, identification run 3 had the lowest final residual of all the runs that were performed. However, some parameters seem to have higher absolute errors when compared to the reference parameters. This result is the consequence of the noise and uncertainty propagation throughout the whole identification process when using DIC and experimental images. The results could also be improved by using more virtual fields, as previous research has shown that the number of virtual fields has a significant impact on the performance of VFM identification, with the number of virtual fields increasing the accuracy of the identification [28]. Fig. 4 shows the evolution of the residual between internal and external virtual works during the identification procedure, as well as a comparison of the external virtual work and the final calibrated internal virtual work for each identification run.

The evolution of the residual during the identification process (Fig. 4a) shows that the initial parameters set have a significant impact on the initial and final calibrated residual values, and consequently, on the identification results. The difference in the final residuals between the identification runs, on the other hand, is small, as can be seen in the difference between the external and virtual works (Fig. 4b), where all the curves are nearly coincident. The small difference in

residuals with the variation of the identified parameters also suggests the need for more virtual fields to be used in the identification process, as using just one virtual field could filter out crucial kinematic data about the mechanical behaviour related to a particular constitutive parameter.

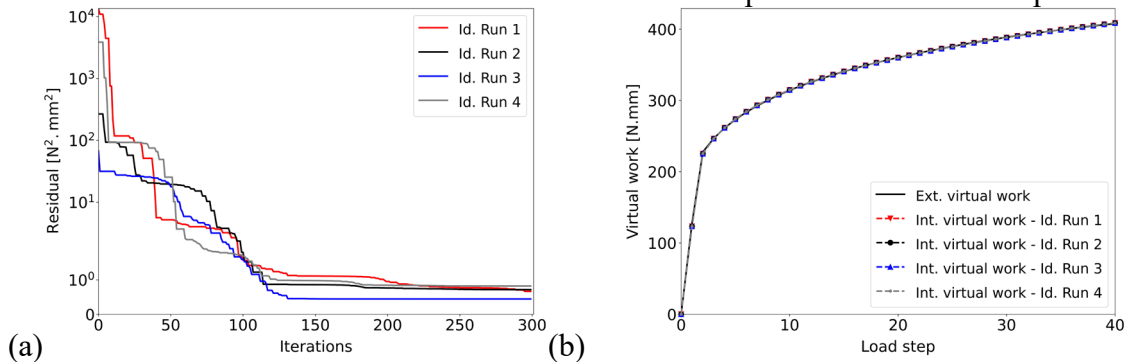


Fig. 4. Identification results in terms of: (a) evolution of the residual during the identification process and (b) final difference between external and internal virtual works.

In Fig. 5, the Swift hardening law curves and the Hill'48 yield surfaces are compared as part of cross-validation between the reference parameters and the identification results. The numerical results for this test configuration are also plotted in the normalised stress space (see Fig. 5b), with the yield stress calculated from the reference parameters.

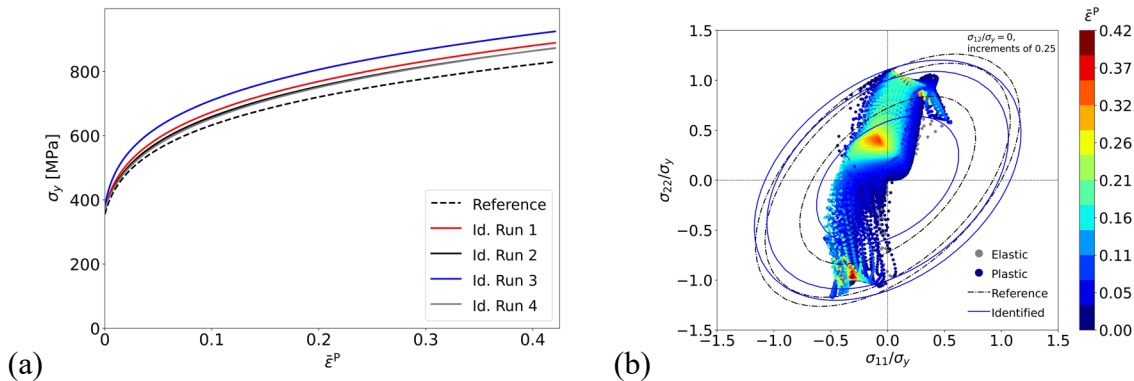


Fig. 5. Results obtained with the identified parameter sets for: (a) Swift law hardening curve for all identification runs and (b) comparison of the reference yield surface with the identified yield surface for the identification run 3 for different levels of σ_{12}/σ_y .

The identified Swift hardening law curves present some divergences from the hardening curve with the reference parameters. These differences become more pronounced as the equivalent plastic strain increases. These results seem to be a consequence of the overall uncertainty propagation in the identification process, in which the global minimum of the residual between the external and internal virtual works may differ from the ground truth parameters due to experimental image noise and the DIC technique's different filtering and spatial resolution. Nevertheless, increasing the number of virtual fields used, even if they are uniform, may improve the accuracy of the parameters identified. Moreover, when comparing the reference and the identification run with the lower residual value (identification run 3), the differences appear to be larger where there is a lack of information in the stress space and lower where there is a higher concentration of points in the stress space. These results are consistent with the previous qualitative analysis of the rotation angle, which revealed a narrower distribution of the rotation angle criterion for this test configuration. A heterogeneous distribution of material points across the whole stress

space would almost certainly improve the accuracy of the identified parameters regarding the anisotropic yield criterion.

Summary

This work investigated the use of different indicators to evaluate the heterogeneity of the mechanical behaviour of distinct test configurations when using the Arcan test. The numerical results from the most interesting test configuration were used to generate synthetic speckle images and processed through DIC and further used in the inverse identification with VFM. The main conclusions that can be drawn from this work are as follows:

- Even with a simple specimen geometry, the Arcan test provided interesting heterogeneous test configurations, demonstrating the potential of its use for heterogeneous test design in the context of metal plasticity.
- The IT_1 criterion proved to be a good quantitative evaluation of the diversity of the material's stress/strain states, which appears to have a significant influence on the inverse identification of the hardening parameters. It is, however, inappropriate for quantifying the identifiability of anisotropy parameters.
- The rotation angle parameter seems to be a suitable qualitative criterion for the evaluation of the sensitivity of mechanical tests to anisotropy.
- When using experimental images and DIC, the propagation of noise and uncertainty throughout the identification process has a significant impact on the identified parameters, resulting in deviations from the ground-truth parameters.

In future works, other test configurations could be used for the inverse identification of the isotropic hardening and anisotropic yielding parameters by finding a good balance between the IT_1 and the rotation angle criterions. Additionally, a greater number of uniform virtual fields could be used in the inverse identification of the constitutive parameters, as could automatic virtual field selection strategies such as sensitivity-based virtual fields. Other specimen geometries could also be used to increase the heterogeneity of stress/strain states of the material, which might become even more important when using more complex constitutive models, such as Yld2000-2D.

Acknowledgements

J. Henriques is grateful to the Portuguese Foundation for Science and Technology (FCT) for the Ph.D. grant 2021.05692.BD. This project has received funding from the Research Fund for Coal and Steel under grant agreement No 888153. The authors gratefully acknowledge the financial support of the FCT under the project PTDC/EMEAPL/29713/2017 by UE/FEDER through the programs CENTRO 2020 and COMPETE 2020, and UID/EMS/ 00481/2013-FCT under CENTRO-01-0145-FEDER-022083. The authors also acknowledge the FCT (FCT - MCTES) for its financial support via the projects UIDB/00667/2020 (UNIDEMI).

Disclaimer

The results reflect only the authors' view, and the European Commission is not responsible for any use that may be made of the information it contains.

References

- [1] A. Lattanzi, F. Barlat, F. Pierron, A. Marek, M. Rossi, Inverse identification strategies for the characterization of transformation-based anisotropic plasticity models with the non-linear VFM, *Int. J. Mech. Sci.* 173 (2020) 105422. <https://doi.org/10.1016/j.ijmecsci.2020.105422>
- [2] P.D. Wu, S.R. MacEwen, D.J. Lloyd, M. Jain, P. Tugcu, K.W. Neale, On pre-straining and the evolution of material anisotropy in sheet metals, *Int. J. Plast.* 21 (2005) 723-739. <https://doi.org/10.1016/j.ijplas.2004.05.007>

- [3] J.M.P. Martins, A. Andrade-Campos, S. Thuillier, Calibration of anisotropic plasticity models using a biaxial test and the virtual fields method, *Int. J. Solids Struct.* 172 (2019) 21-37. <https://doi.org/10.1016/j.ijsolstr.2019.05.019>
- [4] N. Souto, S. Thuillier, A. Andrade-Campos, Design of an indicator to characterize and classify mechanical tests for sheet metals, *Int. J. Mech. Sci.* 101-102 (2015) 252-271. <https://doi.org/10.1016/j.ijmecsci.2015.07.026>
- [5] M. Sutton, J. Orteu, H. Schreier, Image correlation for shape, motion and deformation measurements: basic concepts, theory and applications, first ed., Springer, New York, 2009. <https://doi.org/10.1007/978-0-387-78747-3>
- [6] F. Pierron, M. Grédiac, Towards Material Testing 2.0. A review of test design for identification of constitutive parameters from full-field measurements, *Strain* 57 (2021) 12370. <https://doi.org/10.1111/str.12370>
- [7] F. Pierron, M. Grédiac, The virtual fields method. Extracting constitutive mechanical parameters from full-field deformation measurements, first ed., Springer, New York, 2012. <https://doi.org/10.1007/978-1-4614-1824-5>
- [8] J. Henriques, J. Xavier, A. Andrade-Campos, Identification of Orthotropic Elastic Properties of Wood by a Synthetic Image Approach Based on Digital Image Correlation, *Materials* 15 (2022) 625. <https://doi.org/10.3390/ma15020625>
- [9] J. Aquino, A. Andrade-Campos, J.M.P. Martins, S. Thuillier, Design of heterogeneous mechanical tests: Numerical methodology and experimental validation, *Strain* 55 (2019) 12313. <https://doi.org/10.1111/str.12313>
- [10] J. Fu, W. Xie, L. Qi, An Identification Method for Anisotropic Plastic Constitutive Parameters of Sheet Metals, *Procedia Manuf.* 47 (2020) 812-815. <https://doi.org/10.1016/j.promfg.2020.04.251>
- [11] T. Pottier, P. Vacher, F. Toussaint, H. Louche, T. Coudert, Out-of-plane Testing Procedure for Inverse Identification Purpose: Application in Sheet Metal Plasticity, *Exp. Mech.* 52 (2012) 951-963. <https://doi.org/10.1007/s11340-011-9555-3>
- [12] M. Conde, Y. Zhang, J. Henriques, S. Coppieters, A. Andrade-Campos, Design and validation of a heterogeneous interior notched specimen for inverse material parameter identification, *Finite. Elem. Anal. Des.* 214 (2023) 103866. <https://doi.org/10.1016/j.finel.2022.103866>
- [13] M. Gonçalves, A. Andrade-Campos, B. Barroqueiro, On the design of mechanical heterogeneous specimens using multilevel topology optimization, *Adv. Eng. Softw.* 175 (2023) 103314. <https://doi.org/10.1016/j.advengsoft.2022.103314>
- [14] L. Chamoin, C. Jailin, M. Diaz, L. Quesada, Coupling between topology optimization and digital image correlation for the design of specimen dedicated to selected material parameters identification, *Int. J. Solids. Struct.* 193-194 (2020) 270-286. <https://doi.org/10.1016/j.ijsolstr.2020.02.032>
- [15] P. Wang, F. Pierron, O.T. Thomsen, Identification of Material Parameters of PVC Foams using Digital Image Correlation and the Virtual Fields Method, *Exp. Mech.* 53 (2013) 1001-1015. <https://doi.org/10.1007/s11340-012-9703-4>
- [16] P. Wang, F. Pierron, M. Rossi, P. Lava, O.T. Thomsen, Optimised Experimental Characterisation of Polymeric Foam Material Using DIC and the Virtual Fields Method, *Strain* 52 (2016) 59-79. <https://doi.org/10.1111/str.12170>
- [17] M. Shifa, Strength of Aluminum Alloys Under Static Mixed-Mode I/II Loading Conditions, *J. Test. Eval.* 46 (2018) 294-304. <https://doi.org/10.1520/JTE20160475>
- [18] A. Kumar, M.K. Singha, V. Tiwari, Structural response of metal sheets under combined shear and tension, *Structures* 26 (2020) 915-933. <https://doi.org/10.1016/j.istruc.2020.05.006>

- [19] F. Ozturk, S. Toros, S. Kilic, Effects of Anisotropic Yield Functions on Prediction of Forming Limit Diagrams of DP600 Advanced High Strength Steel, *Procedia Eng.* 81 (2014) 760-765. <https://doi.org/10.1016/j.proeng.2014.10.073>
- [20] Dassault Systèmes. Abaqus 2017 documentation, 2017
- [21] R. Hill, A theory of the yielding and plastic flow of anisotropic metals, *Proc. R. Soc. Lond. A* 193 (1948) 281-297. <https://doi.org/10.1098/rspa.1948.0045>
- [22] H. Takizawa, T. Kuwabara, K. Oide, J. Yoshida, Development of the subroutine library 'UMMDp' for anisotropic yield functions commonly applicable to commercial FEM codes, *J. Phys.: Conf. Ser.* 734 (2016) 032028. <https://doi.org/10.1088/1742-6596/734/3/032028>
- [23] M. Guimarães Oliveira, S. Thuillier, A. Andrade-Campos, Analysis of Heterogeneous Tests for Sheet Metal Mechanical Behavior, *Procedia Manuf.* 47 (2020) 831-838. <https://doi.org/10.1016/j.promfg.2020.04.259>
- [24] MatchID: Metrology beyond colors. MatchID version 2022.2, 2022.
- [25] J. Henriques, M. Conde, A. Andrade-Campos, J. Xavier, Identification of Swift Law Parameters Using FEMU by a Synthetic Image DIC-Based Approach, *Key Eng. Mater.* 926 (2022) 2211-2221. <https://doi.org/10.4028/p-33un7m>
- [26] S. Avril, M. Grédiac, F. Pierron, Sensitivity of the virtual fields method to noisy data, *Comput. Mech.* 34 (2004) 439-452. <https://doi.org/10.1007/s00466-004-0589-6>
- [27] A. Marek, F.M. Davis, F. Pierron, Sensitivity-based virtual fields for the non-linear virtual fields method, *Comput. Mech.* 60 (2017) 409-43. <https://doi.org/10.1007/s00466-017-1411-6>
- [28] J.M.P. Martins, S. Thuillier, A. Andrade-Campos, Calibration of Anisotropic Plasticity Models with an Optimized Heterogeneous Test and the Virtual Fields Method, *Residual Stress, Thermomechanics & Infrared Imaging and Inverse Problems* 6 (2020) 25-32. https://doi.org/10.1007/978-3-030-30098-2_5